

Reconstruction of Hualca Hualca volcano (southern Peru) based on geomorphological and geological evidence and $^{40}\text{Ar}/^{39}\text{Ar}$ dating

J. Alcalá-Reygosa^{a,*}, J.L. Macías^b, J.L. Arce^c, J.C. Gómez^d, G. Cisneros Máximo^b, P.W. Layer^e, J.J. Zamorano^f

^a Departamento de Geografía, Facultad de Filosofía y Letras, Universidad Autónoma de Madrid, Calle Francisco Tomas y Valiente, 1, Campus de Cantoblanco, 28049 Madrid, Spain

^b Instituto de Geofísica, Unidad Michoacán, Universidad Nacional Autónoma de México, Antigua Carretera a Pátzcuaro 8701, 58190 Morelia, Michoacán, Mexico

^c Instituto de Geología, Universidad Nacional Autónoma de México, Coyoacan, 04510 Ciudad de México, Mexico

^d Instituto Geofísico del Perú, Calatrava 216, La Molina, Lima 12, Peru

^e College of Natural Science, Mathematics and Geophysical Institute, University of Alaska Fairbanks, Fairbanks 99775, AK, United States

^f Instituto de Geografía, Universidad Nacional Autónoma de México, Ciudad Universitaria, 04510 Ciudad de México, Mexico

ARTICLE INFO

Keywords:

Hualca Hualca
Central Andes
 $^{40}\text{Ar}/^{39}\text{Ar}$ dating
Geological mapping
Geomorphology
Geochemistry

ABSTRACT

The volcanic history of many of the western Central Andes volcanoes, including Hualca Hualca in the northern Ampato Volcanic Complex, remains poorly constrained. Based on an updated 1:50,000-scale geological map, new cross-sections of the Ampato Complex, a compilation of published dates, new geochemical data and $^{40}\text{Ar}/^{39}\text{Ar}$ ages, we present new insights into its volcanic evolution. Our study identifies 7 principal geological units (4 were not reported on the previous geologic map) and 8, mostly constructive, volcanic phases. The $^{40}\text{Ar}/^{39}\text{Ar}$ dating supports that Hualca Hualca began its formation during the Early Pleistocene (>1.6 Ma) with the establishment of an ancient stratovolcano. This volcano underwent a massive sector collapse to the north that created a U-shaped large amphitheater. This collapse likely resulted in the temporary damming of the Colca River, though no dates or associated deposits have been identified. Subsequent eruptions led to the formation of a smaller volcano along the amphitheater's scar that emplaced andesitic and dacitic lavas. This volcano dubbed modern Hualca Hualca holds the main summit. One of the longest lavas of this edifice reach the Colca valley and was previously dated at 610 ka. Sometime around 550 ka, volcanic activity migrated to the interior of the amphitheater forming the Nevado de Puye, Cruz del Condor, and Ahuashune domes that produced lavas of andesitic and dacitic composition. Around 164 ka a dacitic lava flow was emitted between Nevado del Puye and the base of the modern Hualca Hualca inside the horseshoe crater. The youngest known collapse of the Hualca Hualca complex involved parts of Nevado de Puye dome and the modern Hualca Hualca volcano, emplacing a debris avalanche that again dammed the Colca River and formed an upstream temporary lake that emplaced lacustrine and volcaniclastic deposits. After this collapse, no other volcanic deposit of the Hualca Hualca complex has been identified. Subsequently, glacial erosion during the local Last Glacial Maximum (17–16 ka) modified the volcanic landscape. Geochemical characteristics of Hualca Hualca suggest that their magmas were produced in a metasomatized mantle wedge and likely underwent crustal contamination during their ascent through the thick continental crust.

1. Introduction

Volcanic landforms derive from constructive and destructive processes due to endogenous and exogenous factors, mainly magma composition, eruption style, climate, and tectonic (Thouret, 1999; Grosse et al., 2009; Bustos et al., 2020). Their morphological analysis

combined with geological and geochronologic data, as well as field observations, constitute a key issue for reconstructing the volcanic history that allows us to evaluate the occurrence of future eruptions and to assess the potential hazards and risks for neighboring populations. However, the eruptive chronology of many active and dormant volcanoes throughout the Central Andes is poorly constrained because

* Corresponding author.

E-mail address: jesus.alcala@uam.es (J. Alcalá-Reygosa).

<https://doi.org/10.1016/j.geomorph.2024.109288>

Received 2 November 2023; Received in revised form 16 May 2024; Accepted 1 June 2024

Available online 3 June 2024

0169-555X/© 2024 The Authors. Published by Elsevier B.V. This is an open access article under the CC BY-NC license (<http://creativecommons.org/licenses/by-nc/4.0/>).

many deposits and landforms remain undated. In this sense, a main limitation is the absence of organic matter in the deposits which prevents the use of radiocarbon dating, one of the most used methods in volcanic stratigraphy for the Holocene-Late Pleistocene times. Furthermore, geological and geomorphological approaches in the Central Andes are scarce despite the great diversity of geological sequences and landforms, together with some volcanoes being located in remote areas (Alcalá-Reygosa et al., 2016; Samaniego et al., 2016). A notable example is the Hualca Hualca volcano, which belongs to the Ampato Volcanic Complex (hereafter, AVC), located 70 km northwest of Arequipa City, southern Peru (Fig. 1A). This Complex consists of three successive stratovolcanoes, which from oldest to youngest, are: Hualca Hualca, Ampato, and Sabancaya (Fig. 1B) (Alcalá-Reygosa et al., 2016). In the north, the AVC borders Colca Canyon, with its important agricultural and tourism activities. This canyon is part of the recently established Colca and Volcanes of Andagua Geopark, and therefore, a major effort is needed to assess its geohazard potential. It should be noted that most of the volcanic reconstruction effort (chronology, geochemical evolution etc.) in the AVC is focused on the Sabancaya and Ampato volcanoes. For instance, Samaniego et al. (2016) provided the largest dataset of lava ages, pyroclastic deposits, and peatbogs from both edifices based on ^{40}K – ^{40}Ar , radiocarbon, and in situ-produced cosmogenic ^3He dating. Furthermore, a few in situ-produced cosmogenic ages (^3He) were obtained from lavas (Bromley et al., 2019). By contrast, Hualca Hualca still presents many relevant unresolved issues such as: (i) the geological map has not been updated, thus, some observed geological units are not represented in the current map; (ii) its age, chemical composition, and volcanic evolution are poorly constrained; (iii) the ages of some significant events, such as the collapse of the northern flank of the volcano, are not well-constrained; and (iv) there has been no geomorphological analysis of the volcano based on stratigraphic and morphologic relationship.

In this study, we provide an update of the geological map—previously generated by the Instituto Geológico Minero y Metalúrgico de Peru (2001)—with new ^{40}Ar – ^{39}Ar ages and geochemical data from lavas emitted on the northern flank of Hualca Hualca volcano. With this information and a new geomorphological cross-section traced on the geomorphological map published by Alcalá-Reygosa et al. (2016), we propose a general evolution of the volcano that is characterized by eight volcanic phases, with one of the most significant being a massive volcanic collapse that affected the oldest part of the edifice.

2. Regional setting

The western Central Andes resulted from the subduction of the Nazca Plate beneath the South American Plate (e.g. Stern, 2004), generating widespread volcanism as Quaternary-Holocene composite volcanoes, caldera systems, and monogenetic volcanic fields (e.g. Allmendinger et al., 1997). One of the largest volcanic systems is the AVC, which covers an area of 630 km². It is comprised by three coalescent stratovolcanoes: Hualca Hualca, Sabancaya, and Ampato. Hualca Hualca is the northernmost stratovolcano of the AVC (15°24'–15°51' S/ 71°51'–73°W; 6025 m asl), being bound in the north by the deeply incised Colca River (3500 m asl), to the west by the surrounding Altiplano (4000 m asl), and to the south by the Sabancaya (5992 m asl) and Ampato (6288 m asl) volcanoes. According to previous studies, the formation of Hualca Hualca took place during the Late Pliocene and Early Pleistocene (Gerbe and Thouret, 2004). It is composed of andesitic rocks and exhibits a horseshoe-shaped scarp produced by the collapse of its northern flank toward the Colca Canyon (Palacios and Klinck, 1988). Afterwards, glacial processes affected the volcano, thereby emplacing extensive moraine deposits and polished and striated rock surfaces (Alcalá-Reygosa et al., 2017). The formation of the southern Ampato volcano started 450 ka ago and has a relatively young summit dated at 20–10 ka (Samaniego et al., 2016). Sabancaya volcano is the youngest structure of the AVC with Holocene and modern eruptions (Gerbe and Thouret,

2004).

The climate of the western Central Andes is modulated by the Intertropical Convergence Zone. The wet season occurs from December to March, when the Intertropical Convergence Zone shifts southwards, recording 70–90 % of the annual precipitation (800–1000 mm) (Dornbusch, 1998; Herreros et al., 2009). Humid air masses from the Pacific Ocean rarely affect the study area because a persistent temperature inversion layer exists at 800 m asl, caused by atmospheric subsidence conditions and the Humboldt Current (Rutllant and Ulriksen, 1979; Garreaud et al., 2003). Temperatures are homogeneous during the year as suggested by the mean annual air temperature records (4.36 °C at 4850 m asl) from the Chachani volcanic complex (16°03'–16°20'S/ 71°39'–71°25' W; 6057 m asl) (Andrés et al., 2011).

3. Methods

3.1. Geomorphological cross-section

A geomorphological map (1:20,000 scale) of the AVC was published by Alcalá-Reygosa et al. (2016). This map classifies relief based on morphogenetical and morphochronological criteria using several colors in addition to areal, lineal, and point symbols. It shows the detailed distribution of volcanic, glacial, periglacial, fluvial, lacustrine, and gravitational landforms and their relative chronological order. Building upon their work, we generate an N-S geomorphological cross-section from Hualca Hualca to Ampato volcano crossing the most significant geomorphological units. In this way we present an in-depth relative evolutionary reconstruction of the AVC. Our analysis of the geomorphological cross-section distinguishes coherent relief formation stages, which can be constructive or destructive. Constructive phases involve effusive and explosive volcanic activity whereas destructive phases include explosive, gravitational, or erosion processes that have deteriorated or dismantled the original volcanic relief.

3.2. Geological mapping

Based on the geological map of the Instituto Geológico, Minero y Metalúrgico de Peru (INGEMMET, 2001) (Fig. 2), in addition to published literature and fieldwork campaigns, we have updated the geologic map (1:50,000 scale) of the Hualca Hualca volcano. The first step was georeferencing the previous INGEMMET geologic map with ArcGIS 10.2 software using the WGS-1984-UTM-Zone-19S coordinate system. Separately, we obtained 1:20,000 scale (12.5 m contour interval) topographic maps from the Instituto Geográfico de Peru, as well as Advanced Land Observing Satellite (ALOS) images provided by the Alaska Satellite Facility (ASF). We then imported the topographic data into the Ilwis 3.3 commercial software package to construct a 12.5-m²-resolution DEM with x-y-z coordinates. Next, we interpolated a point network layer with a 12.5-m² resolution (ALOS-ASF) in ArcGIS to construct several thematic maps (slope, dissection, and altitude). We imported all of this information into Ilwis 3.3 to generate anaglyph images that were then used to analyze lithological and geomorphological contacts among volcanic landforms and faults. Later, we verified the map using several fieldwork campaigns performed in 2003, and from 2011 to 2017.

We obtained the areas and volumes of the main units with the 3D Analyst automated tool module of the Geographical Information System ©ArcGIS 10.2. The module calculates the volumetric difference between two surfaces, the current DEM (upper) and a hypothetical lower triangulated of which (TIN) anchored to the base of the geological unit (the most feasible paleosurface). Each surface model consists of individual cells of which the module integrates the approximate volume between the lower (z-base), and the upper surface of the analyzed area (z-top). The maximum lengths of lavas were taken from the topmost part of the associated dome.

During fieldwork, we defined lithological contacts, and description of major stratigraphic units of the volcano. We also collected rock

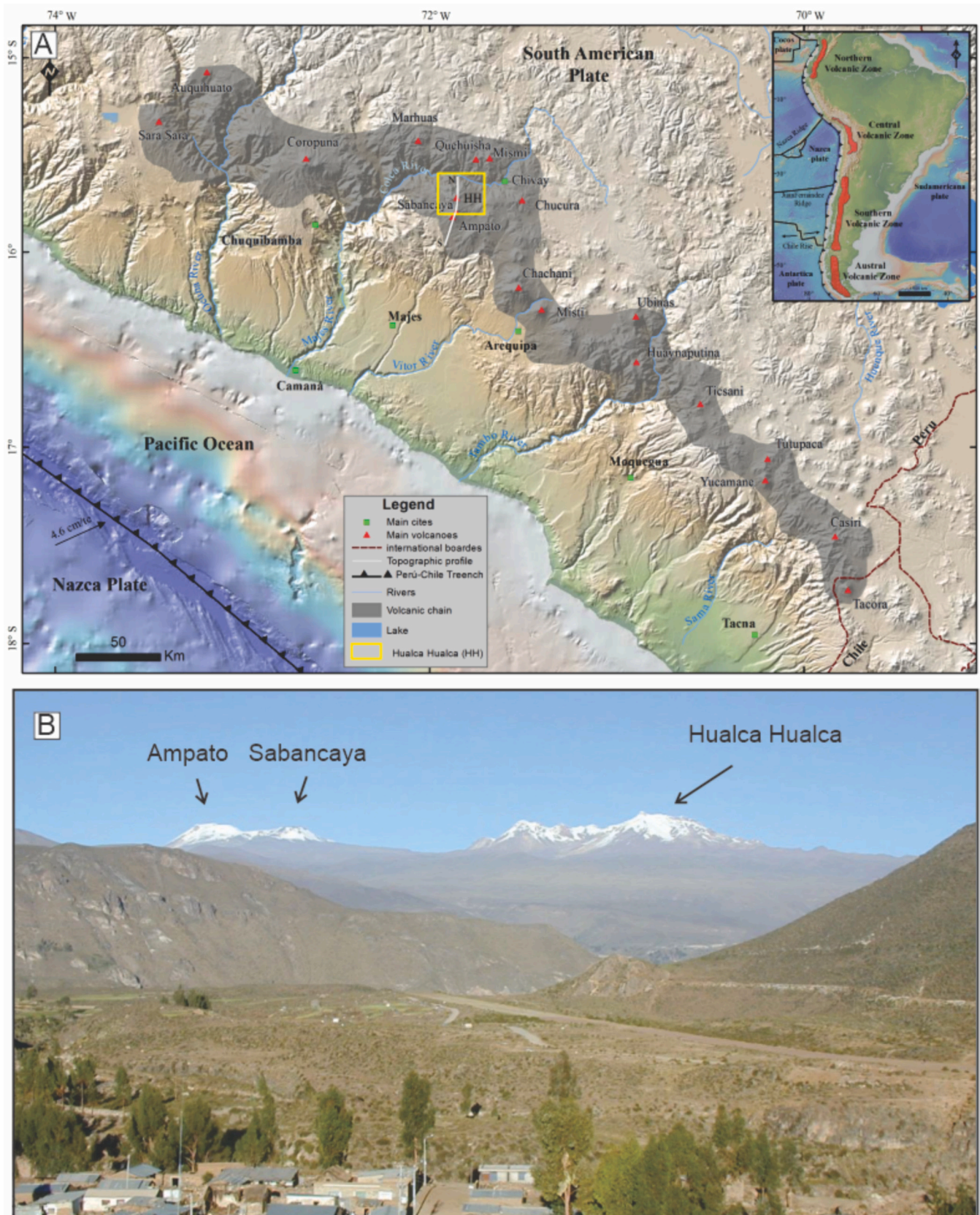


Fig. 1. A) Location of the Ampato Volcanic Complex (AVC; 6288 m asl), in the western Central Andes. This volcanic range resulted from the subduction of the Nazca Plate beneath the South American Plate (Central Volcanic Zone in inset). The yellow box represents the AVC and the white line the geomorphological profile of Fig. 6. B) View from the northeast of the snowcapped AVC; from the left to the right appear Ampato, Sabancaya, and Hualca Hualca volcanoes. (For interpretation of the references to colour in this figure legend, the reader is referred to the web version of this article.) Photograph taken from the village of Chivay.

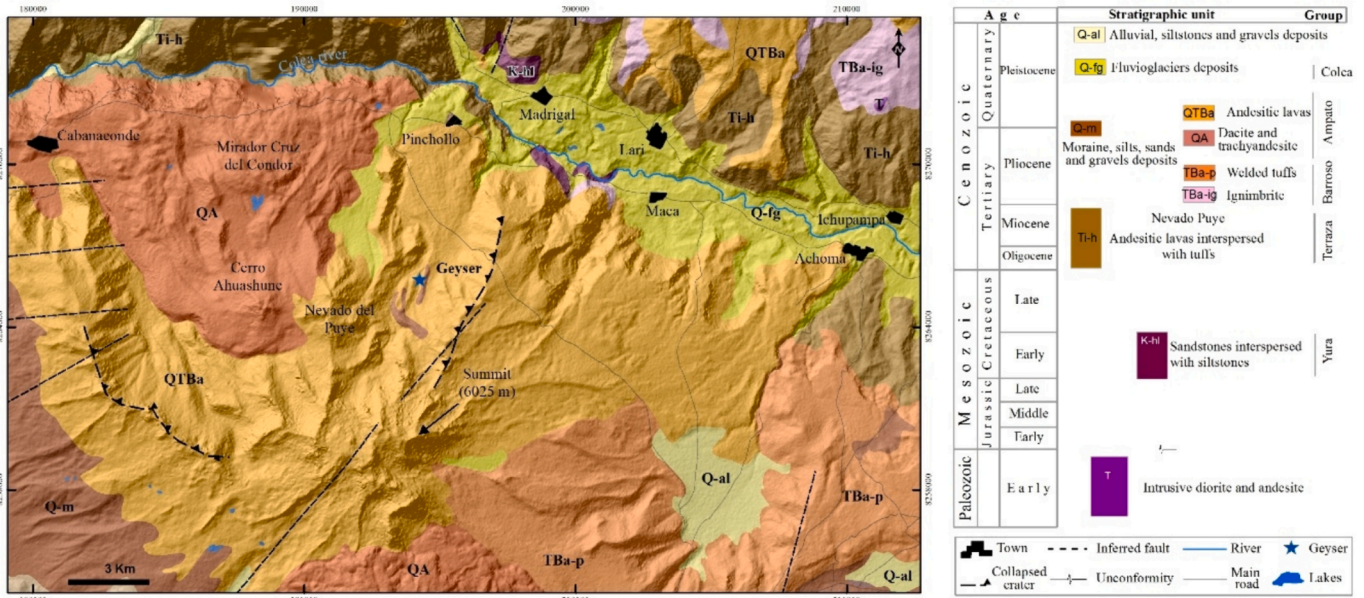


Fig. 2. Geological map of Hualca Hualca volcano and surrounding areas according to INGEMMET (2001). Abbreviations of volcanic structures are: NP = Nevado de Puye, CA = Cerro Ahuashune, and MC = Mirador Cruz del Condor.

samples for petrographic and geochemical analysis and $^{40}\text{Ar}/^{39}\text{Ar}$ dating. The new map of Hualca Hualca (Fig. 3) displays 17 geological units that are described in the accompanied stratigraphic column, in addition to the ages of moraine deposits obtained using the ^{36}Cl method from Alcalá-Reygosa et al. (2017), and the locations of the rock samples collected for petrographic and geochemical analysis.

3.3. $^{40}\text{Ar}/^{39}\text{Ar}$ dating

We selected fresh rock samples to use the $^{40}\text{Ar}/^{39}\text{Ar}$ method at the Geochronology Lab, University of Alaska, Fairbanks. Only three samples were appropriate for analysis, they were collected from two lavas of the Nevado Puye and one more from the Ancient Hualca structures (Table 1). The analyses were conducted by laser step-heating of phenocryst-free groundmass rock fragments, following the procedures outlined in Layer (2000) and Layer et al. (2009). The mineral TCR-2

with an age of 28.6 Ma (Renne et al., 2010), was used to monitor neutron flux and to calculate the irradiation parameter J , for all samples. The measured argon isotopes for system blank and mass discrimination, and for the irradiated samples, calcium, potassium, and chlorine interference reactions were corrected following the procedures of McDougall and Harrison (1999). The $^{40}\text{Ar}/^{39}\text{Ar}$ ages were calculated using the constants of Renne et al. (2010) and are reported at the 1-sigma level. Typical full-system, fifteen-minute laser blank values (in moles), were generally 6×10^{-16} mol ^{40}Ar , 3×10^{-18} mol ^{39}Ar , 3×10^{-18} mol ^{38}Ar , and 1×10^{-17} mol ^{36}Ar , which are 10 to 50 times smaller than the sample/standard volume fractions. Mass discrimination was monitored by running calibrated air shots. The mass discrimination during this method was 1.0 % per mass unit. We performed two runs for each sample, with the most precise run being chosen for the presentation and discussion. A sample is considered to have a plateau if it has 3 or more contiguous fractions, constituting at least 50 % ^{39}Ar release, while being

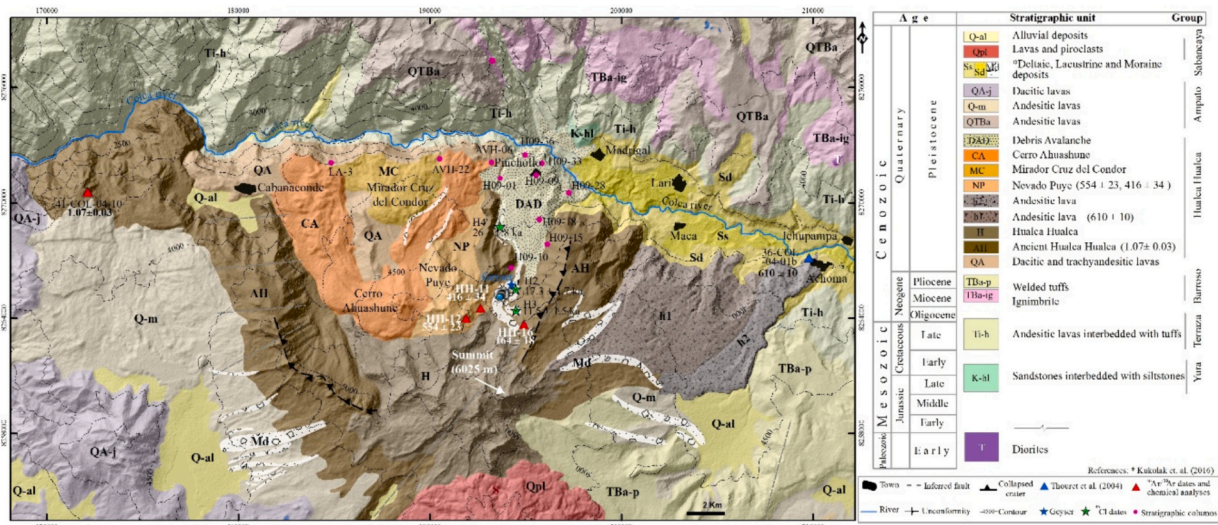


Fig. 3. Updated geological map of Hualca Hualca volcano and the surrounding area showing the new $^{40}\text{Ar}/^{39}\text{Ar}$ of rock samples and previous ^{36}Cl ages dates obtained on moraines (Alcalá-Reygosa et al., 2017). Notice the new geologic contour lines of the Nevado de Puye (NP), Cerro Ahuashune (CA), and Mirador Cruz del Condor (MC) volcanic structures that are exposed inside the collapsed structure.

Table 1
Summary of ⁴⁰Ar/³⁹Ar analysis from Hualca Hualca samples. Whole-rock (WR) of each sample was analyzed. Because the samples have evidence of excess argon, the isochron ages are preferred. For the three samples, multiple runs were done and the best age is a composite isochron age. MSWD, mean square weighted deviates.

| Sample | Min. | Integrated age (ka) | Plateau age (ka) | Plateau information | Isochron age (ka) | Isochron information |
|-----------|-----------|---------------------|------------------|---|-------------------|--|
| Hualca-11 | WR run #1 | 863 ± 64 | 619 ± 133 | 3 of 7 fractions 79 % ³⁹ Ar release MSWD = 5.11 | 466 ± 36 | 7 of 7 fractions ⁴⁰ Ar/ ³⁶ Ar _i = 300 ± 1 MSWD = 0.95 |
| | WR run #2 | 1182 ± 93 | 480 ± 54 | 4 of 9 fractions 78 % ³⁹ Ar release MSWD = 0.37 | 315 ± 55 | 9 of 9 fractions ⁴⁰ Ar/ ³⁶ Ar _i = 303 ± 1 MSWD = 0.70 |
| | 2 runs | | | | 416 ± 34 | 16 of 16 fractions ⁴⁰ Ar/ ³⁶ Ar _i = 301 ± 1 MSWD = 1.24 |
| Hualca-12 | WR run #1 | 691 ± 40 | 585 ± 39 | 3 of 7 fractions 68 % ³⁹ Ar release MSWD = 0.15 | 543 ± 41 | 7 of 7 fractions ⁴⁰ Ar/ ³⁶ Ar _i = 300 ± 1 MSWD = 0.87 |
| | WR run #2 | 763 ± 43 | 608 ± 25 | 4 of 9 fractions 65 % ³⁹ Ar release MSWD = 0.33 | 557 ± 32 | 9 of 9 fractions ⁴⁰ Ar/ ³⁶ Ar _i = 299 ± 1 MSWD = 1.22 |
| | 2 runs | | | | 554 ± 23 | 16 of 16 fractions ⁴⁰ Ar/ ³⁶ Ar _i = 299 ± 1 MSWD = 0.94 |
| Hualca-16 | WR run #1 | 225 ± 46 | 259 ± 26 | 6 of 7 fractions 96 % ³⁹ Ar release MSWD = 1.28 | 242 ± 25 | 7 of 7 fractions ⁴⁰ Ar/ ³⁶ Ar _i = 294 ± 2 MSWD = 1.23 |
| | WR run #2 | 202 ± 32 | 124 ± 22 | 5 of 10 fractions 93 % ³⁹ Ar release MSWD = 0.39 | 128 ± 17 | 10 of 10 fractions ⁴⁰ Ar/ ³⁶ Ar _i = 299 ± 1 MSWD = 0.42 |
| | 2 runs | | | | 164 ± 18 | 17 of 17 fractions ⁴⁰ Ar/ ³⁶ Ar _i = 298 ± 1 MSWD = 1.68 |

significant at the 95 % confidence level (as indicated by Mean Square Weighted Deviates; MSWD < ~2.5).

3.4. Geochemical analysis

We selected fresh samples for whole-rock chemical analysis. Unfortunately, only four rock samples were analyzed for geochemistry, two lava samples of the NP, one from AH, and another one for H units (Table 2). We selected the less weathered samples for these analyses. Rock fragments were cleaned and washed, then powdered with stainless steel disks. We analyzed major elements using X-Ray Fluorescence at the Laboratorio Nacional de Geoquímica y Mineralogía (Universidad Nacional Autónoma de México, México). Further details can be found in Lozano-Santacruz and Bernal (2005). Trace elements, including rare

earth elements, were measured by Inductively Coupled Plasma Mass Spectrometry (ICP-MS) at Activation Labs, Ontario, Canada, following the protocols described at <https://actlabs.com>, and at the Laboratorio de Estudios Isotópicos, Centro de Geociencias, Juriquilla (Universidad Nacional Autónoma de México, México). See Mori et al. (2007) for analytical procedures.

4. Results

4.1. Geological map

A geological map of the AVC was presented by INGEMET in 2001 (Fig. 2). In this map, Hualca Hualca volcano displays two main lithological units: Pliocene andesitic lavas (QTba) at the base and Pleistocene

Table 2
Whole-rock chemical analysis of different units from Hualca Hualca volcano. Major elements analyzed by XRF are reported in wt%, and trace elements were analyzed by ICP-MS are reported in ppm. Total Fe reported as Fe2O3. Units are: AH, Ancient Hualca; H, Hualca Hualca, NP, Nepopualco (see Fig. 3).

| Sample | Unit | SiO ₂ | TiO ₂ | Al ₂ O ₃ | F ₂ O ₃ t | MnO | MgO | CaO | Na ₂ O | K ₂ O | P ₂ O ₅ | Total | Li | Be | Sc | V | Cr |
|--------|------|------------------|------------------|--------------------------------|---------------------------------|------|------|------|-------------------|------------------|-------------------------------|-------|------|-----|------|-----|------|
| H09-15 | AH | 59.25 | 1.05 | 17.14 | 6.73 | 0.07 | 2.89 | 5.34 | 4.28 | 2.83 | 0.39 | 100.2 | 12.5 | 1.7 | 10.3 | 155 | 73.1 |
| H09-2 | H | 63.36 | 0.79 | 15.49 | 4.82 | 0.05 | 2.15 | 3.96 | 4.16 | 3.76 | 0.27 | 100.2 | 16.6 | 2.1 | 7.5 | 102 | 50.4 |
| HH-11 | NP | 60.78 | 0.92 | 15.77 | 5.57 | 0.08 | 2.75 | 4.81 | 3.59 | 2.95 | 0.33 | 99.6 | | 2 | 9.9 | 124 | 43 |
| HH-12 | NP | 63.66 | 0.71 | 15.58 | 6.16 | 0.16 | 2.16 | 3.67 | 3.69 | 3.12 | 0.25 | 100.0 | | 2 | 7.7 | 89 | 41 |

| Sample | Unit | Co | Ni | Cu | Zn | Rb | Sr | Y | Zr | Cs | Ba | La | Ce | Pr | Nd | Sm | Eu |
|--------|------|------|------|------|------|------|-----|------|-----|-----|------|------|------|------|------|-----|-----|
| H09-15 | AH | 19.9 | 36.4 | 58.2 | 90.4 | 73.3 | 660 | 14.6 | 198 | 1.1 | 939 | 35.6 | 60.9 | 9.4 | 32.5 | 5.8 | 1.5 |
| H09-2 | H | 13.1 | 22.8 | 22.1 | 74.0 | 84.7 | 568 | 13.3 | 111 | 3.1 | 897 | 40.2 | 68.0 | 10.0 | 33.2 | 5.7 | 1.2 |
| HH-11 | NP | 16.9 | 27 | 56 | 75 | 93 | 774 | 11 | 199 | 0.7 | 1035 | 45 | 82 | | 38 | 6 | 1.4 |
| HH-12 | NP | 16.3 | 32 | 30 | 91 | 104 | 652 | 12 | 218 | 0.8 | 1116 | 49 | 89 | | 40 | 5.7 | 1.3 |

| Sample | Unit | Gd | Tb | Dy | Ho | Er | Tm | Yb | Lu | Hf | Ta | Pb | Th | U |
|--------|------|-----|------|------|------|------|------|------|------|-----|-----|------|------|-----|
| H09-15 | AH | 4.3 | 0.62 | 2.89 | 0.50 | 1.30 | 0.18 | 1.14 | 0.16 | 5.4 | 0.5 | 14.3 | 7.4 | 1.4 |
| H09-2 | H | 4.0 | 0.56 | 2.58 | 0.45 | 1.19 | 0.18 | 1.13 | 0.16 | 3.7 | 0.7 | 18.7 | 14.9 | 2.8 |
| HH-11 | NP | | 0.5 | | | | | 1 | 0.16 | 5.1 | 0.7 | 17 | 10.7 | 2.5 |
| HH-12 | NP | | 0.6 | | | | | 0.98 | 0.15 | 5.5 | 0.7 | 6 | 12.3 | 3 |

trachyandesite and dacitic lavas on top (QA). The map did not include the absolute ages of both units that were covered either by morainic (Qm), fluvioglacier (Qfg), and alluvial (Qal) deposits. The updated version of the Hualca Hualca geological map (Fig. 3) uses the cartographic contours of Paleozoic and Mesozoic rocks provided by INGEMET (2001), absolute ages of two lavas (Thouret et al., 2007), moraines (Alcalá-Reygosa et al., 2016), and new $^{40}\text{Ar}/^{39}\text{Ar}$ dates of the four samples collected during our fieldwork campaigns. The unit limits were refined with the interpretation of an anaglyph image.

Based on all this information, we divided the geology of the volcano into the following units, from base to top:

- QA unit is exposed as an isolated area in the central part of the amphitheater of Hualca Hualca and on the upper part of the southern wall of the Colca River, including the village of Cabanaconde. The lithology comprises reddish to dark gray trachyandesite and dacitic lavas. This unit corresponds to the same QA unit of INGEMET (2001) but with a restricted distribution.
- AH unit is composed of a series of andesitic lavas that form the ancient part of the volcano. They are well-exposed on the inner walls of the amphitheater/scar (Fig. 4), covering a minimum exposed area of 176 km² with a total volume of 24.3 km³. A sample from the lava of the AH unit located on the western slopes of the volcano, outside the amphitheater/scar, was dated by Thouret et al. (2004, 2007) at 1.07 ± 0.03 Ma. In the INGEMET (2001) map, AH corresponds to the Pliocene QTBa. This unit was present previous to the volcano collapse.
- H unit consists of a succession of andesites and dacitic lavas that disrupt and bisect the amphitheater/scar of AH. This unit contains

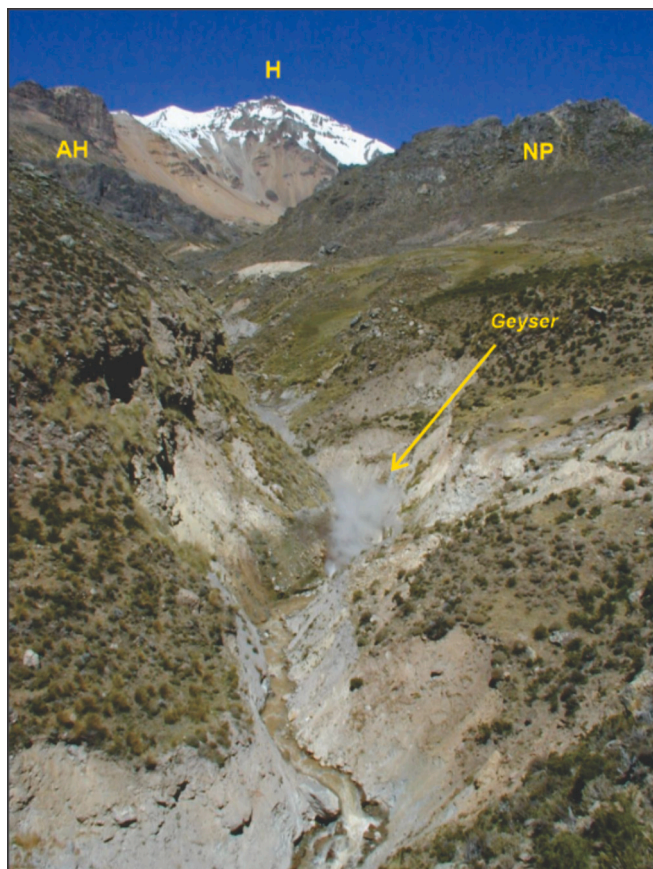


Fig. 4. View looking south of the summit of Hualca Hualca volcano (H). In the background, parts of the layered lavas of the Ancient Hualca Hualca (AH), and the dome and lavas of Nevado de Puye (NP) can be observed.

the topmost part of the volcano, which is highly altered and hosts glacier remnants (Fig. 4). H covers a minimum exposed area of 67 km² with a total volume of 10 km³. At least two sequences of lavas extend to the northeast h1 (~15 km) toward the village of Maca, and to east-northeast h2 (~17 km) toward the village of Achoma. H2 is an andesitic lava on top of older lacustrine sediments (QTBa unit) exposed in the outskirts of Achoma (Fig. 5A). A rock of h2 unit was also dated by Palacios and Klinck (1988) at 0.9 ± 0.2 Ma using the K—Ar method. Another sample of this unit was dated by Thouret et al. (2004, 2007) at 0.61 ± 0.01 Ma using the $^{40}\text{Ar}/^{39}\text{Ar}$ method. It should be noted that H2 was included in the QTBa unit of INGEMET (2001).

- Nevado de Puye unit (NP), is located inside the amphitheater toward the eastern part. It consists of a partly disrupted dome structure with a maximum elevation of 5310 m and lavas that extend to the north. NP covers an area of 18.24 km² with an estimated volume of 1.58 km³. The rocks are andesitic lavas made of phenocryst of plagioclase and pyroxene as observed at sites HH-11 and HH-12 (Fig. 4).
- MC unit is situated inside the amphitheater toward the central part of HH and close to the Colca River canyon, covering the lavas of the QA unit. It consists of a series of domes and lavas with a maximum elevation of 4440 m. Measured from the topmost part of the dome, these lavas have maximum lengths between 3.5 and 2.5 km close to the famous sight “Mirador Cruz del Condor” (Fig. 5B). MC covers an area of 14.6 km² with a minimum exposed volume of 0.6 km³.
- Cerro Ahuashune unit (CA) is located inside the amphitheater of HH toward the western part. It consists of a dome structure with a maximum elevation of 5190 m and lavas that extend to the northwest for at least 10 km and to the north-northeast for ca. 8 km. CA covers an area of 52.5 km² with an estimated volume of 4.8 km³. A rock sample of this unit was dated at 0.6 ± 0.3 Ma using the K—Ar method by Palacios and Klinck (1988).
- DAD unit is extended across the northeastern part of HH inside the amphitheater, close to Pinchollo and Madrigal villages, which are located on the southern and northern parts of Colca Canyon. The unit is exposed across an area of around 19.1 km² and has a minimum volume of 1 km³. It appears as a massive heterolithologic deposit with a jigsaw-fit structure. The age of this debris avalanche must be younger than unit H (0.6 Ma; Thouret et al., 2007) because it was affected by the collapse.
- Moraine deposits appear in all the flanks of HH, distinguishing inner, lateral, and frontal moraines and morainic crests. They are located between 3650 m asl and close to the glaciers that cover the summit. The moraine record occurs as single ridges or ridge complexes showing most of them as voluminous and well-preserved morphologies. The use of ^{36}Cl exposure surface dating displayed in Fig. 3, revealed that these morainic deposits were formed at 17–16 ka and 12 ka (Alcalá-Reygosa et al., 2017).

4.2. Volcanic reconstruction based on geomorphological criteria

Our geomorphological cross section (Fig. 6) traced on the geomorphological map published by Alcalá-Reygosa et al. (2016) indicates that the Hualca Hualca volcano is the oldest edifice of the AVC. Based on this geomorphology, we identified eight volcanic phases of the volcano, seven of them constructive (phases I, II, IV, V, VI, VII) and at least one destructive (phase III). Therefore, Ampato volcano formed during seven phases, producing mixed (effusive and explosive) eruptions. Based on our geomorphological cross-section, it is evident that the initial stages of Ampato overlap with the latest stages of the construction of Hualca Hualca. Sabancaya volcano is the youngest edifice of the complex, consisting of eight phases, mostly effusive.

Hualca Hualca volcano has a maximum elevation of 5190 m in contrast with the minimum elevation of 3000 m at the base of the Colca River valley. The main feature of the Hualca Hualca edifice is a ~14 km

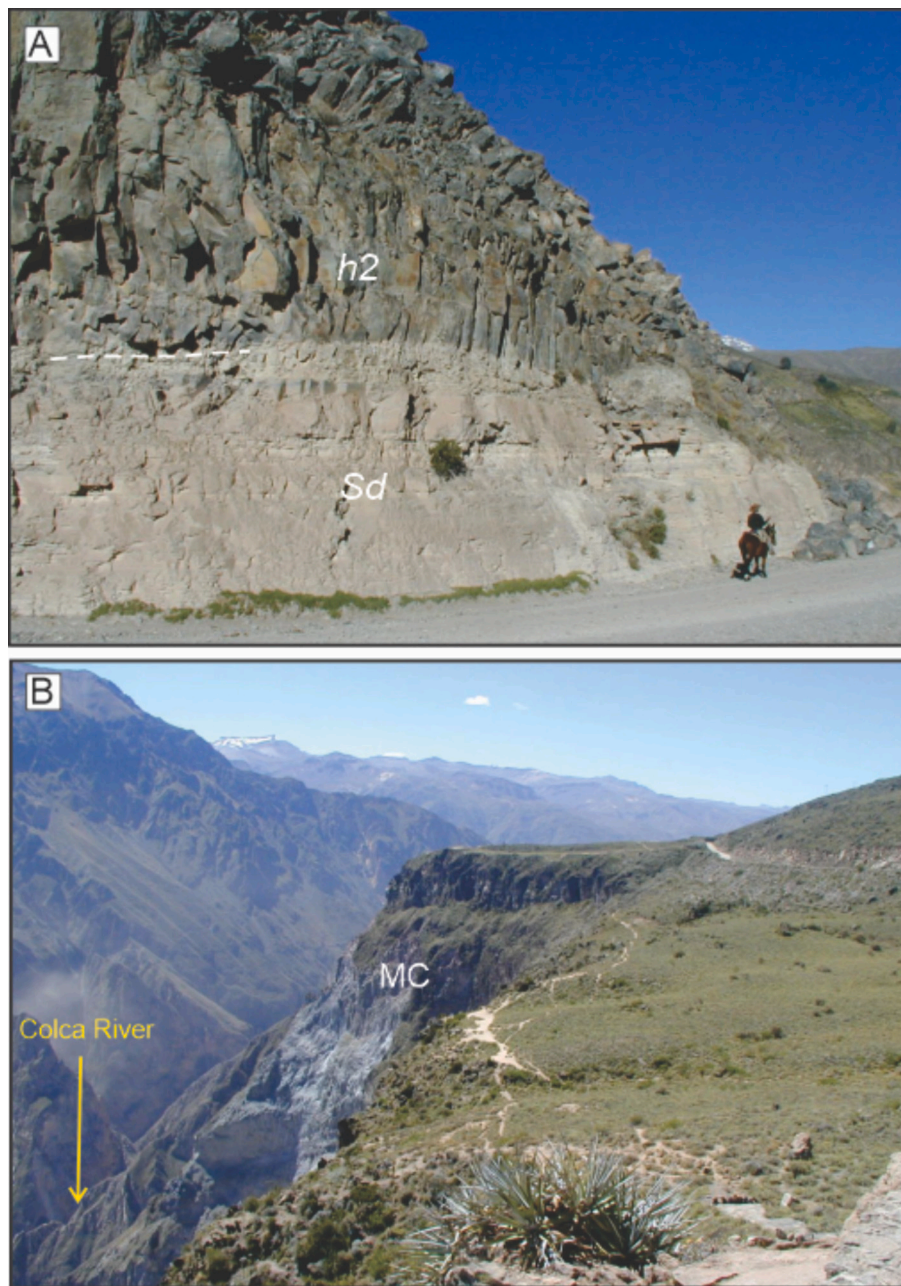


Fig. 5. A) View from the northeast of the andesitic lava h2 on top of sedimentary layers along the Achoma Maca dirt road, B) View from the west of the Cruz del Condor site to Colca Canyon with the lavas of the MC unit exposed at the upper part of the cliff.

semicircular scar that cuts the volcano summit. As a consequence, the external flanks of the volcano have slopes varying from 8° to 67° , whereas the internal slopes are steeper, ranging from 38° up to 82° . This scar exposes the internal volcanic structure mainly composed of a succession of stacked lavas (Fig. 4). Within the scar, at elevations between 3780 and 4350 m, lava domes occur in addition to lavas that were intensively affected by glaciers during the last glacial cycle. Our geomorphological and geological analysis suggests that the scar is not entirely associated with a widespread collapse of the northern flank of the volcano as previously suggested, because only a localized debris avalanche deposit is confined to the eastern part of Hualca Hualca (Gómez et al., 2004), as presented in Fig. 3. This deposit has a minimum extension of ~ 12 km and exhibits hummocky topography.

4.3. $^{40}\text{Ar}/^{39}\text{Ar}$ dating

We collected four rock samples for $^{40}\text{Ar}/^{39}\text{Ar}$ dating at the Hualca Hualca to determine the age of the volcano (Fig. 3 and Table 2). Two rock samples were taken in the Nevado de Puye unit (NP), inside the scar collapse, which yielded isochron ages of 554 ± 23 and 416 ± 34 ka (Fig. 7). Another sample was collected from the eastern scarp of Hualca Hualca, which yields an isochron age of 164 ± 18 ka (Fig. 7). The last sample was collected from a debris avalanche deposit exposed to the north of Colca River.

4.4. Geochemical analysis

We used a database of chemical analyses from the AVC (Samaniego et al., 2016) that has just been augmented by Rivera et al. (2023). Four rock samples were analyzed to determine the chemical composition of

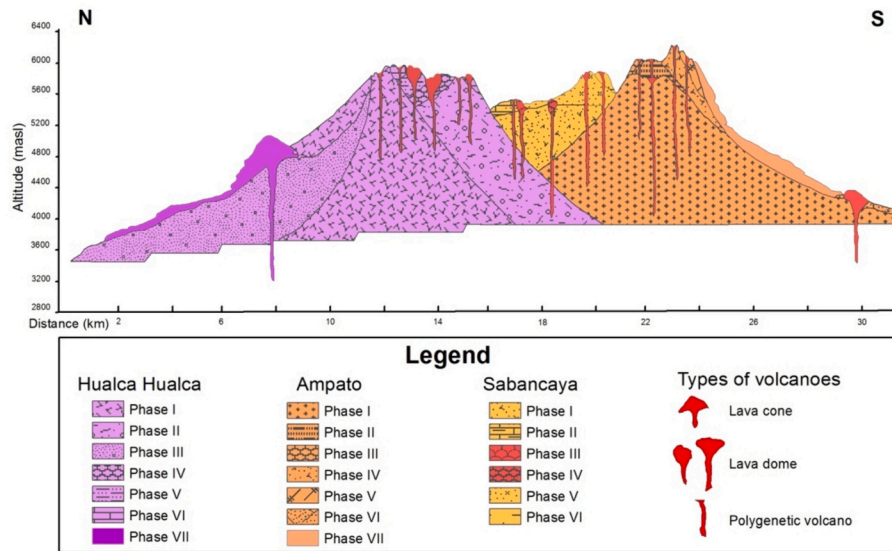


Fig. 6. N-S geomorphological cross-section of the AVC traced on the geomorphological map published by Alcalá-Reygosa et al. (2016).

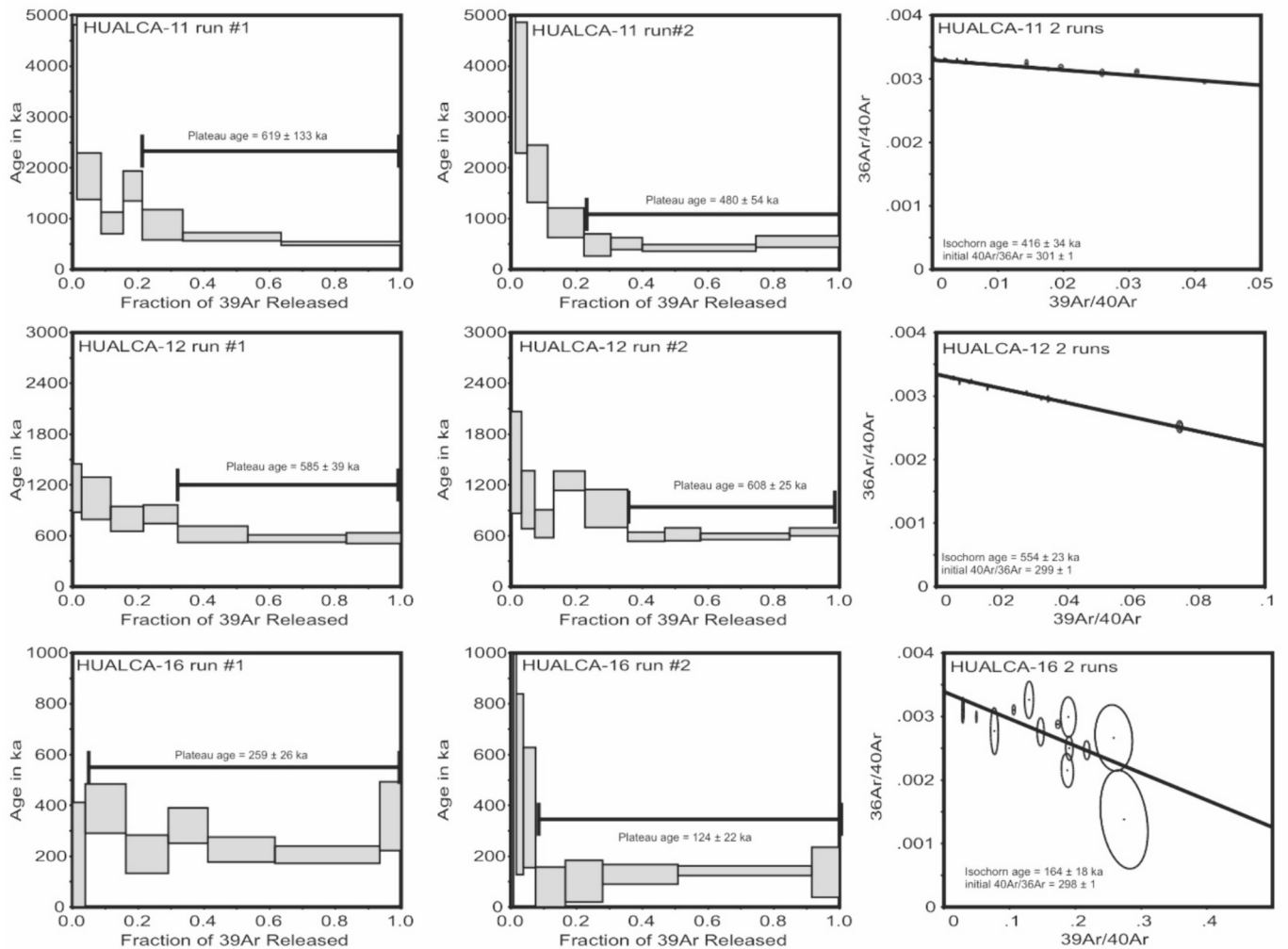


Fig. 7. $^{40}\text{Ar}/^{39}\text{Ar}$ plateau and isochron ages of the selected samples from Hualca Hualca volcano. The results are quoted to the ± 1 sigma level and are calculated using the constants of Steiger and Jäger (1977).

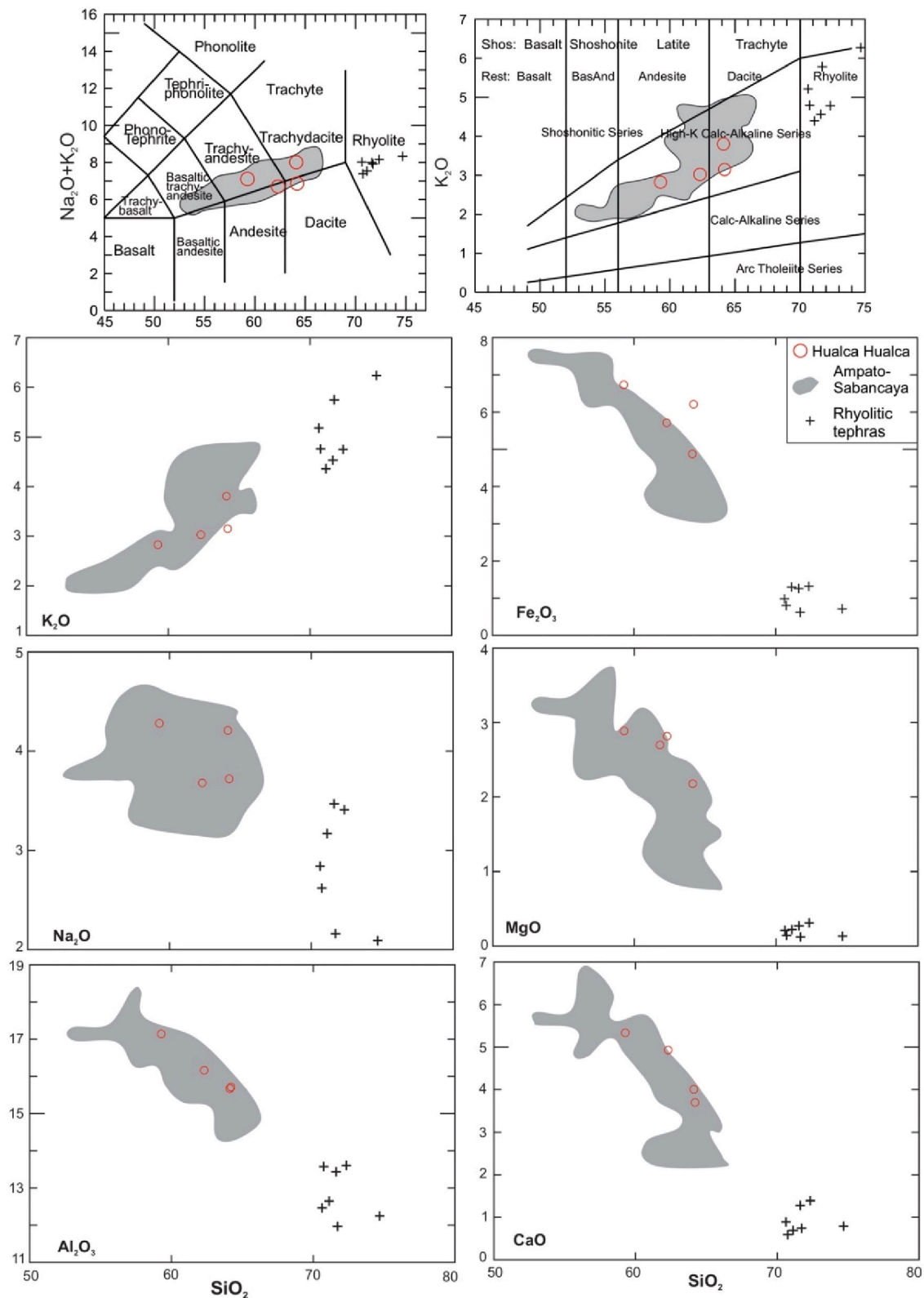


Fig. 8. A) Chemical classification of total alkalis vs major elements (Le Bas et al., 1986; Peccerillo and Taylor, 1976) and binary diagrams of Hualca Hualca, Ampato, and Sabancaya stratovolcanoes. DAD = debris avalanche deposit from Hualca Hualca. Gray area and rhyolitic samples from Samaniego et al. (2016) and Rivera et al. (2023).

the Hualca Hualca edifice, which varies from trachyandesite to trachydacite within the high-K calc-alkaline series (Fig. 8). Silica compositions for the four samples range from 54 to 59 wt% and 6.8–8.0 wt% in alkalis. The andesites and dacites from Hualca Hualca fit well with the andesites and dacites of Sabancaya-Ampato database (Fig. 8). One exception is the rhyolitic samples reported for the basal Ampato (rhyolitic tephtras) with >75.5 wt% SiO₂ that are not linearly correlated with the rest of the samples (Rivera et al., 2023). The three edifices of the AVC are classified as high-K calc-alkaline rocks (Fig. 8), with the Ampato Upper samples

having a wider compositional range. Major elements of rock samples from Hualca Hualca volcano are also similar to andesites and dacites from the Sabancaya and Ampato volcanoes (Fig. 8). All data displays clear negative trends for MgO, Fe₂O₃, CaO, P₂O₅, Al₂O₃, and TiO₂, and a weak negative correlation in Na₂O. Only K₂O shows a positive correlation. Beyond the few data available for Hualca Hualca volcano, we can say that such trends could indicate a common magmatic source for the entire volcanic complex (the three volcanic structures), although negative correlations are suggesting the fractionation of mafic mineral

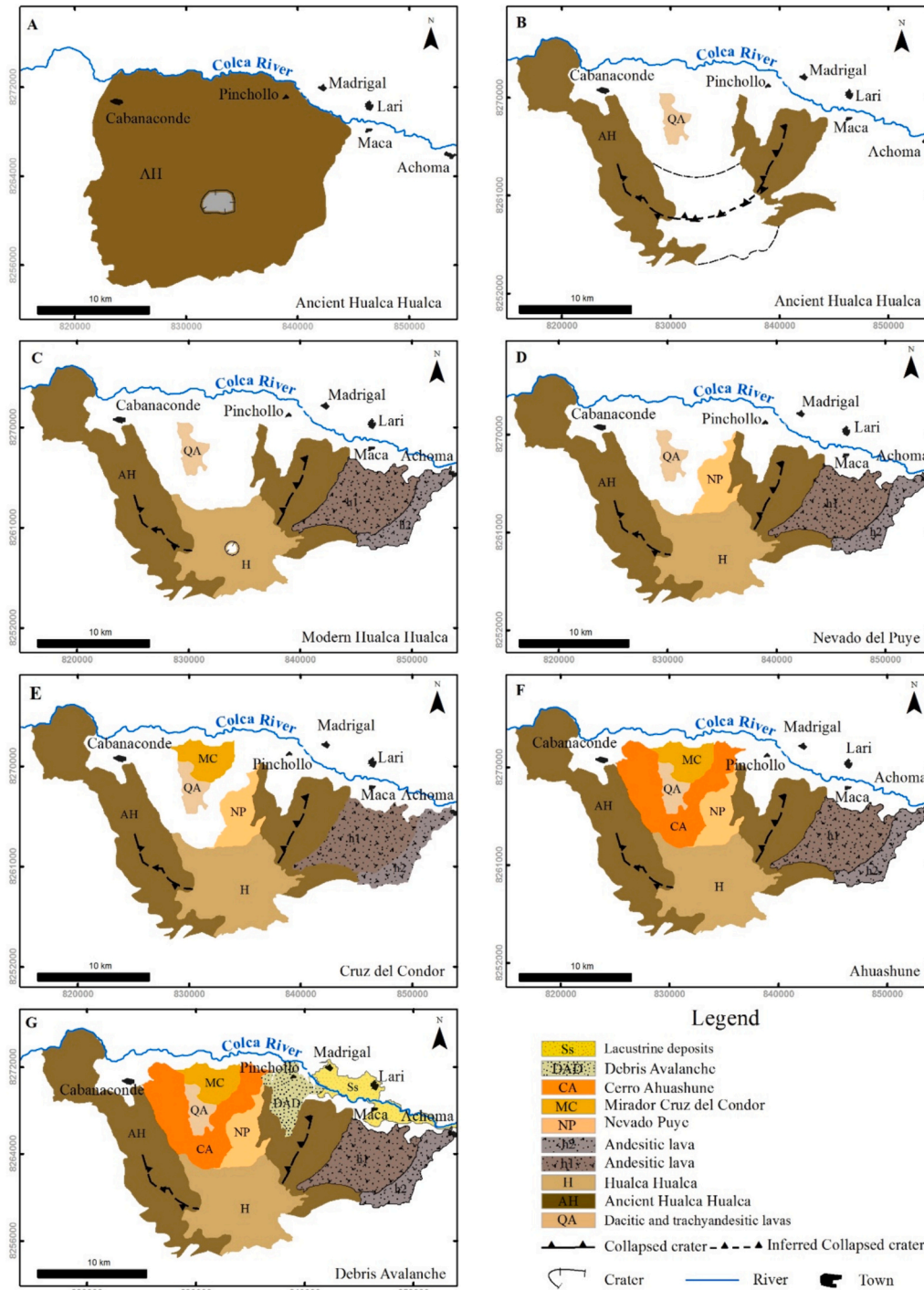


Fig. 9. A–B) Sketch showing the evolution of the Ancient Hualca Hualca volcano that was destroyed by a major sector collapse. C) A modern edifice was built at the collapse crater dispersing lava flows (e.g. h1 and h2). D–F) Afterward, three successive lava dome edifices were emplaced inside the amphitheater, and finally G) a younger collapse disrupted the inner part of the edifice forming a debris avalanche deposit that blocked the Colca River.

phases (olivine, pyroxene) as well as calcic plagioclase and amphibole. Thus, this positive trend could be produced by the same process (Wilson, 1989).

5. Discussion

5.1. Evaluation of the updated geological map of Hualca Hualca volcano

The new geological map of Hualca Hualca (1:50,000 scale) defines seven main units, labeled from base to top: QA, AH, H, NP, MC, CA, and DAD (Fig. 3). Some units have basically the same extension as those presented in the map of INGEMET (2001), such as MC and QA. However, several limits have been improved. One of the main findings of the new version of the Hualca Hualca geological map is the identification of new geological units such as AH, H, H1, and H2. Thus, this new map of the Hualca Hualca volcano—aided by geomorphological, geochemical, and geochronological data—sheds new light on its evolution. The presented map, together with the updated map of Ampato and Sabancaya volcanoes presented by Rivera et al. (2023), gives a more comprehensive view of the evolution of the volcanic complex and the series of volcanic and geological hazards in the region.

5.2. Overview of the Hualca Hualca evolution

The Hualca Hualca volcano had been classified as an extinct volcano (INGEMET, 2001). In our study, the volcano appears as a Pliocene to Early Pleistocene edifice composed of andesitic, dacite, and trachyandesite lavas (Figs. 2 and 3). In their detailed K—Ar geochronological study of Colca Canyon, Thouret et al. (2007) dated lava samples exposed on the western flank of the Ancient Hualca Hualca volcano that yielded an age of 1.6 Ma. This is the oldest age reported so far of the volcano which confirms a Pleistocene age for the ancient edifice (AH). This volcano was constructed through the emission of andesitic lavas that formed a central edifice (Fig. 9A). Several of these lavas are exposed on the amphitheater's inner walls and at the Colca River canyon on top of the late Jurassic sedimentary rocks (K—hl) and late Cretaceous to Oligocene volcanic rocks (Ti—h). The distribution of these lavas in the north of Pinchollo area should have blocked the river and formed temporary lakes followed by voluminous debris flows downstream. To have a rough estimation of the area covered by this ancient volcano and its volume, we traced a hypothetical baseline for the volcano that yields a minimum exposed area of 176 km² with a total volume of 160 km³. This ancient edifice dominated the region because neither Ampato nor Sabancaya volcanoes had been formed. Ancient Hualca Hualca (AH) was interrupted by the collapse of the volcano toward the north generating a horseshoe crater open to the north (Fig. 9B). This collapse destroyed the ancient edifice and left a wide scar that today is ~1.6 km long and represents the main geomorphological feature of the volcano. This whole scar has been associated with the collapse of Hualca Hualca that emplaced a debris avalanche deposit that blocked the Colca River forming an upstream lake until the village of Chivay (Palacios and Klinck, 1988). However, mapping and fieldwork led Gomez et al. (2004) to restrict this debris avalanche deposit to the northeast part of the ancient volcano scar, as shown in Fig. 3. Therefore, the large amphitheater is not associated with this debris avalanche (DAD unit in the map) deposit but rather with an older deposit that has not been described yet. A detailed geochronological study of the volcanic succession is still missing, and the oldest products of the volcano have not yet been dated.

After this major collapse of the ancient edifice (AH) the volcanic activity recommenced at the horseshoe crater forming a modern Hualca Hualca volcano (H unit) through the emission of radial lava flows that covered ca. 8 km of the collapse scarp. This modern edifice constitutes the main summit of the volcano and the remains of glacier on top (Fig. 3). By looking to the erosion gullies and glacier activity the H edifice has been intensively eroded. A very important morphologic

feature is that the volcano structure is not affected by the horseshoe scarp suggesting that it is younger (Fig. 9C). The furthest lavas that were dispersed by the volcano are the H1 and H2 units located to the east-northeast of the summit. One of these lavas is exposed close to the village of Maca on the southern wall of the Colca River where it covers older partly indurated lacustrine deposits (Fig. 5A) described as Sd in the geological map and mapped by Kukulak et al. (2016). Thouret et al. (2007) dated this lava ~600 ka. Based on the distribution of the products we estimated that this modern volcano (H unit) covered a minimum area of 18 km² and has an original volume larger than 2 km³. Thus, modern Hualca Hualca (H) started its construction following the older failure of the Ancient edifice (AH) of unknown age and continued its activity up to 600 ka. A younger lava collected at the base of the modern Hualca Hualca edifice and east of Nevado del Puye dome (see Fig. 3) was dated in this study at ~164 ka (Table 1). This dacitic lava suggest so far that this activity may have been the youngest volcanic activity of the modern Hualca Hualca volcano.

Around 550 ka, volcanism migrated ~6 km to the north to commence the activity of Nevado del Puye volcanic structure that ended up to 416 ka (Fig. 9D). This activity lasted for about 60 ka, erupted dacitic lavas that flowed toward the north inside the amphitheater and ended with the emplacement of a central dome. The activity resumed ~5.5 km to the northwest with the emission of dacitic lavas that formed a dome complex here called Mirador Cruz del Condor (MC) (Fig. 9E). This dome complex dispersed thick lavas that flowed into the Colca Valley. Finally, the volcanic activity migrated ~3 km to the southwest forming the Ahuashune volcano that dispersed ~10 km long basaltic andesitic lavas surrounding the Mirador Cruz del Condor dome (Fig. 9F). The longest lava flowed between Mirador Cruz del Condor and the western wall of the amphitheater up to the modern skirts of the Cabanaconde village. Palacios and Klinck (1988) dated these lavas at 0.6 ± 0.3 Ma with the K—Ar method. However, based on the lithologic contacts that cover the NP and MC domes we consider that the age of Ahuashune must be younger. Unfortunately, we do not have new dates for these two dome complexes.

A notorious debris avalanche deposit occurs inside the amphitheater between the limits of the Nevado del Puye and the lower horseshoe crater of the Ancient edifice (AH) (Fig. 9G). It extends beyond the Colca River in the outskirts of the Madrigal village. This deposit was originally described by Palacios and Klinck (1988) and reappraised by Avalos et al. (2004). The debris avalanche dammed the Colca River and formed a temporary lake with lacustrine and fluvial sedimentation that today are exposed from Lari and downstream from Chivay. These lacustrine deposits were mapped as deltaic deposits (Ss) by Kukulak et al. (2016) as shown in Fig. 3. The debris dam was eventually broken with the subsequent formation of massive debris flows downstream that may have reached the Pacific Ocean.

This global evolution of Hualca Hualca agrees with the degree of dissection and the morphological characteristics of this edifice compared to Ampato and Sabancaya volcanoes (Figs. 4 and 6). Hence, there is an apparent migration of volcanic activity from the north (Hualca Hualca) to the south (Sabancaya) as it has been stated in previous studies (e.g. Rivera et al., 2023).

According to Samaniego et al. (2016), the oldest rocks of Ampato have been dated at 440 ka, corresponding to the Basal Ampato unit. From a geochemical basis, the linear trends of the total alkalis vs silica diagram and the binary diagrams of the AVC suggest that they are cogenetic and/or the magmas suffered under the same evolutionary process (Fig. 10). Ampato volcano displays a wider compositional range from basic andesites to dacites and Sabancaya's composition ranges from andesites to dacites (Rivera et al., 2023), Hualca Hualca samples reported here being similar to the Sabancaya edifice. However, the trends observed in the binary diagrams are typical evolutive trends that involve crystal fractionation from trachyandesitic up to rhyolitic magmas. Fractionating phases could have been pyroxene, calcic plagioclase, and Fe—Ti oxides that diminish the Fe, Mg, Ca, and Ti contents. The relative

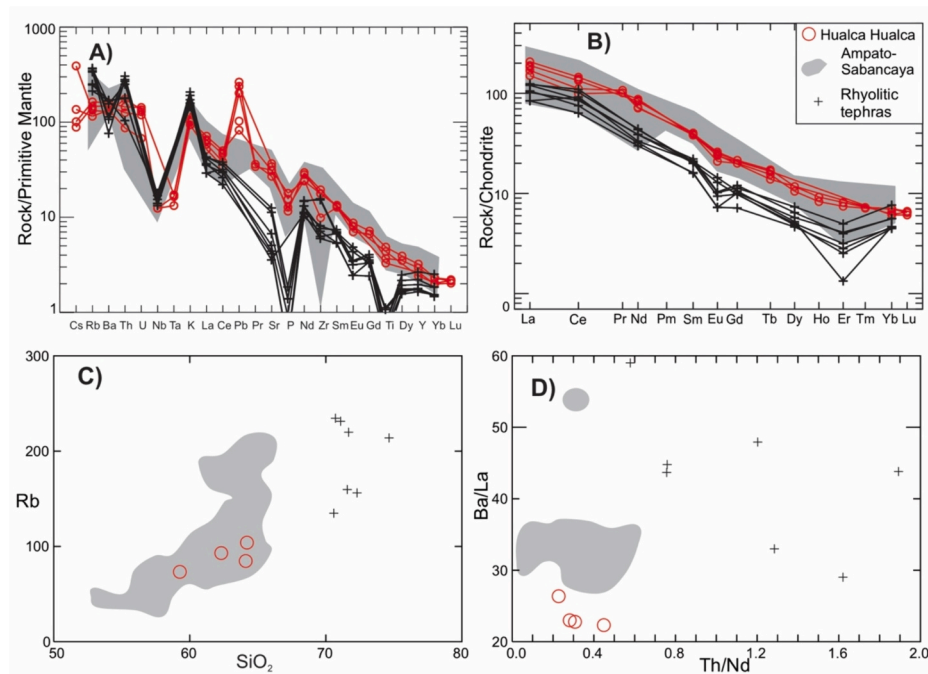


Fig. 10. A) Mantle-normalized and B) Chondrite-normalized trace element concentrations of the Hualca Hualca samples (Sun and McDonough, 1989); C) Silica vs Rb and D) Th/Nd vs Ba/La of the Hualca Hualca samples (including DAD, debris avalanche deposit), compared to the Ampato-Sabancaya compositional field. Gray area and rhyolitic samples are from Samaniego et al. (2016) and Rivera et al. (2023).

enrichment in incompatible compared to less compatible elements as well as light rare earth elements (LREE) compared to heavy rare earth elements (HREE) (Fig. 10A–B), plus the negative anomaly in Nb and Ta, as well as the positive anomaly in Cs, K, and Pb, are all indicative of a subduction environment for the genesis of Hualca Hualca magmas via partial melting of the metasomatized mantle wedge, as suggested by Rivera et al. (2023).

Notably, Hualca Hualca samples show a more pronounced positive Pb anomaly (Fig. 10A), that could be related to a higher degree of subduction component influence. Again, rhyolitic samples display different patterns in the trace element diagrams, particularly the deep negative Sr, P, and Ti anomalies and the low values in most of the REE. An increase in Rb with increasing SiO₂ is expected when a relatively mafic magma evolves into a felsic melt (Wilson, 1989). However, the rhyolitic sample from Sabancaya does not follow this trend (Fig. 10C), suggesting that they were produced by unrelated magmas from the complex. Finally, the ratios Th/Nd vs Ba/La recorded weak influence of fluids from the slab and melts from slab sediments (Pearce, 1982), instead, the geochemical characteristics for the three volcanic structures have been ascribed to complex processes of Assimilation Fractional Crystallization (AFC) in both the lower and upper crust plus mixing (Rivera et al., 2023).

5.3. Geomorphological implications

The massive failure of the northern volcanic flank of the Ancient Hualca Hualca volcano produced important implications for the geomorphology of whole edifice because the failure destroyed a large part of the stratovolcano. The resulting amphitheater has had steep slopes where several glacial, periglacial, and gravitational processes have taken place including the younger and famous debris avalanche deposit that blocked the river and generated a temporary lake preserved up-valley from the modern village of Chivay (Gómez et al., 2004; Alcalá-Reygosa et al., 2016). The debris dam was eventually broken with the subsequent formation of a massive debris flows downstream that may have reached the Pacific Ocean.

The volcanic collapse formed a horseshoe crater with a maximum depth of ~1600 m, presenting a well-defined cirque. Although the amphitheater continued filling, the frequency and magnitude of emissions decreased as shown by the reduced appearance of lava sequences that culminate the morpho-stratigraphic series of the caldera. Most of the lavas and post-caldera eruptive centers show evidence of glacial modifications. This means that all or at least most of these landforms were already fully formed before the local Last Glacial Maximum (17–16 ka) (Alcalá-Reygosa et al., 2017) occurred. For instance, the highest edifices exhibit inactive glacial cirques, corroborating the existence of ice masses after their formation.

6. Conclusions

The combination of a new geological map, geomorphological cross section, geochemical analysis, and ⁴⁰Ar/³⁹Ar dating has been essential to improving the volcanic evolutionary model of Hualca Hualca volcano. The new map shows 7 main geological units, absolute ages, as well as an improved delimitation of morainic, fluvioglacial, and alluvial deposits, where we propose a series of 8 volcanic phases. Thus, Hualca Hualca is considered as the extinct northern part of the AVC, which began its formation during the Pliocene to Early Pleistocene. The volcano represents a good example of ancient edifices that have been affected by major sector collapses. The oldest edifice AH, collapsed >>0.6 Ma affecting its northern flank that formed the amphitheater observed today. Successive activity occurred inside the u-shaped crater forming the Nevado de Puye (554–416 ka), the Mirador Cruz del Condor and the Ahuashune domos and associated lavas. The youngest collapse occurred from the modern edifice HH, inside the AH amphitheater. The collapse formed a debris avalanche that blocked the Colca River in the outskirts of the Madrigal village (Palacios and Klinck, 1988; Avalos et al., 2004). Afterwards, glacial activity during the local Last Glacial Maximum (17–16 ka) changed most of the volcano. Geochemical characteristics of the Hualca Hualca samples are very similar to those reported for Ampato-Sabancaya stratovolcanoes, that were sourced from a metasomatized mantle wedge and then evolved by complex AFC and mixing

processes.

CRediT authorship contribution statement

J. Alcalá-Reygosa: Writing – review & editing, Writing – original draft, Visualization, Validation, Supervision, Methodology, Investigation, Formal analysis, Conceptualization. **J.L. Macías:** Writing – review & editing, Writing – original draft, Visualization, Validation, Supervision, Resources, Project administration, Methodology, Investigation, Funding acquisition, Formal analysis, Conceptualization. **J.L. Arce:** Writing – review & editing, Writing – original draft, Validation, Supervision, Resources, Methodology, Investigation, Formal analysis, Data curation, Conceptualization. **J.C. Gómez:** Writing – review & editing, Writing – original draft, Validation, Methodology, Investigation, Funding acquisition, Formal analysis, Data curation, Conceptualization. **G. Cisneros Máximo:** Writing – review & editing, Writing – original draft, Visualization, Validation, Software, Resources, Methodology, Formal analysis, Data curation. **P.W. Layer:** Writing – review & editing, Writing – original draft, Validation, Methodology, Investigation, Formal analysis, Data curation, Conceptualization. **J.J. Zamorano:** Writing – review & editing, Writing – original draft, Visualization, Methodology, Formal analysis, Data curation.

Declaration of competing interest

The authors declare that they have no known competing financial interests or personal relationships that could have appeared to influence the work reported in this paper.

Data availability

Data will be made available on request.

Acknowledgments

This work was partially supported by 2009 and 2013 grants to J.L. Macías from the Instituto Panamericano de Geografía e Historia (IPGH), the Instituto Geofísico del Perú, and the Instituto de Geofísica of the Universidad Nacional Autónoma de México. This research was also supported by the grant DGAPA-UNAM IN101123 to J.L. Arce. FRX analysis was performed at Laboratorio Nacional de Geoquímica y Mineralogía, UNAM by P. Girón-García and ICP-MS analysis was conducted at Centro de Geociencias, UNAM, Juriquilla, Mexico by O. Pérez Arvizu. Thanks to M.C. Macías-Romo for her support during sample preparation for chemical analysis, Felipe García T. for the preparation of thin sections of collected rocks, and Grant George Buffett for the English edition of the manuscript. We are indebted to two anonymous reviewers who provided very constructive comments of our manuscript. The first author dedicates this work with great affection to his father Felix Alcalá Pascual.

References

- Alcalá-Reygosa, J., Palacios, D., Zamorano, J.J., 2016. Geomorphology of the Ampato volcanic complex (southern Peru). *J. Maps* 12 (5), 1160–1169.
- Alcalá-Reygosa, J., Palacios, D., Vázquez-Selem, L., 2017. A preliminary investigation of the timing of the local last glacial maximum and deglaciation on Hualca Hualca volcano - Patapampa Altiplano (arid Central Andes, Peru). *Quat. Int.* 449, 149–160.
- Allmendinger, R.W., Jordan, T.E., Kay, S.M., Isacks, B.L., 1997. The evolution of the Alti-Plano-Puna plateau of the Central Andes. *Annu. Rev. Earth Planet. Sci.* 25, 139–174.
- Andrés, N., Palacios, D., Úbeda, J., Alcalá, J., 2011. Ground thermal conditions at Chachani Volcano. *Southern Peru. Geografiska Annaler* 93 (3), 151–162.
- Bromley, G.R.M., Thouret, J.C., Schimmelpfennig, L., Mariño, J., Valdivia, D., Rademaker, K., Vivanco Lopez, S.P., Team, A.S.T.E.R., Aumaitre, G., Bourles, D., Keddadouche, K., 2019. In situ cosmogenic ^3He and ^{36}Cl and radiocarbon dating of volcanic deposits refine the Pleistocene and Holocene eruption chronology of SW Peru. *Bull. Volcanol.* 81 (64), 1–16.
- Bustos, E., Arnoso, M., Báez, W., Norini, G., Suzaño, N.O., Viramonte, J.G., 2020. Geomorphological evolution of the Chimpa stratovolcano in the back-arc region of the Central Andes. *Geomorphology* 364, 107251.
- Dornbusch, U., 1998. Current large-scale climatic conditions in Southern Peru and their influence on snowline altitudes. *Erdkunde* 52, 41–54.
- Garreaud, R., Vuille, M., Clement, A.C., 2003. The climate of the Altiplano: observed current conditions and mechanisms of past changes. *Palaeogeogr. Palaeoclimatol. Palaeoecol.* 194, 5–22.
- Gerbe, M.C., Thouret, J.C., 2004. Role of magma mixing in the petrogenesis of tephra erupted during the 1990–98 explosive activity of Nevado Sabancaya, southern Peru. *Bull. Volcanol.* 66, 541–561.
- Gómez, J., Siebe, C., Macías, J.L., Ocola, L., 2004. Debris Avalanche in Hualca Hualca Volcano-Arequipa, Perú. *Penrose Meeting. American Geology Society, Puebla, México*, pp. 313–315.
- Gomez, J.C., Macías, J.L., Siebe, C., Ocola, A.L., 2004. Debris avalanche deposit of Hualca Hualca volcano and the formation of a volcanic dam in the Colca Valley, Arequipa, Peru. *International Association of Volcanology and Chemistry of the Earth Interior General Assembly, Chile*.
- Grosse, P., De Vries, B.V.W., Petrinovic, I.A., Euillades, P.A., Alvarado, G.E., 2009. Morphometry and evolution of arc volcanoes. *Geology* 37 (7), 651–654.
- Herreros, J., Moreno, L., Taupin, J.D., Ginot, P., Patris, N., De Angelis, M., Ledru, M.P., Delachaux, F., Schotterer, U., 2009. Environmental records from temperature glacier ice on Nevado Coropuna saddle, southern Peru. *Adv. Geosci.* 22, 27–34.
- Instituto Geológico Minero y Metalúrgico de Perú. 2001. Mapa geológico del cuadrángulo de Chivay. Escala 1:100,000. INGEMMET, Sector Energía y Minas, Republica del Perú.
- Kukulak, J., Paulo, A., Kalicki, T., 2016. Lithology of lacustrine deposits in the Colca Valley. *J. South Amer. Earth Sci.* 69, 152–170.
- Layer, P.W., 2000. $^{40}\text{Ar}/^{39}\text{Ar}$ age of the El gygytyn impact event, Chukotka, Russia: *Met. Plan. Sc.* 35, 591–599.
- Layer, P.W., García-Palomo, A., Jones, D., Macías, J.L., Arce, J.L., Mora, J.C., 2009. El Chichón volcanic complex, Chiapas, Mexico: Stages of evolution based on field mapping and $^{40}\text{Ar}/^{39}\text{Ar}$ geochronology. *Geof. Int.* 48, 33–54.
- Le Bas, M.J., Le Maitre, R.W., Streckaisen, A., Zanetti, B., 1986. A chemical classification of volcanic rocks based on the total alkali-silica diagram. *J. Pet.* 27, 745–750.
- Lozano-Santacruz, R., Bernal, J.P., 2005. Characterization of a new set of eight geochemical reference materials for XRF major and trace element analysis: *Rev. Mex. Ciencias Geol.* 22, 329–344.
- McDougall, I., Harrison, T.M., 1999. *Geochronology and Thermochronology by the $^{40}\text{Ar}/^{39}\text{Ar}$ Method-2nd Ed.* Oxford University Press, New York, p. 269.
- Mori, L., Gómez-Tuena, A., Cai, Y., Goldstein, S.L., 2007. Effects of prolonged flat subduction on the Miocene magmatic record of the central Trans-Mexican Volcanic Belt. *Chem. Geol.* 244, 452–473.
- Palacios, O., Klinck, B.A., 1988. Evidencias de un embalse volcánico en el valle del Colca. *Boletín de la Sociedad Geológica del Perú* 78, 237–244.
- Pearce, J.A., 1982. Trace element characteristics of lavas from destructive plate boundaries. In: Thorpe, R.S. (Ed.), *Orogenic Andesites and Related Rocks*. John Wiley and Sons, Chichester, England, pp. 528–548.
- Peccerillo, A., Taylor, S.R., 1976. Geochemistry of Eocene calc-alkaline volcanic rocks from Kastamonu area, Northern Turkey. *Contrib. Mineral. Petrol.* 58, 63–81.
- Renne, P.R., Mundil, R., Balco, G., Min, K., Ludwig, K., 2010. Joint determination of ^{40}K decay constants and $^{40}\text{Ar}/^{39}\text{Ar}$ for the fish Canyon sanidine standard and improved accuracy for $^{40}\text{Ar}/^{39}\text{Ar}$ geochronology. *Geochim. Cosmochim. Acta* 74, 5349–5367.
- Rivera, M., Samaniego, P., Nauret, F., Mariño, J., Liorzou, C., 2023. Petrological and geochemical constraints on the magmatic evolution at the Ampato-Sabancaya compound volcano (Peru). *Lithos* 458–459 (5), 107364.
- Rutllant, J., Ulriksen, P., 1979. Boundary layer dynamics of the extremely arid northern part of Chile: the Antofagasta field experiment. *Bound. Layer. Meteorology* 17, 41–55.
- Samaniego, P., Rivera, M., Mariño, J., Guillou, H., Liorzou, C., Zerathe, S., Delgado, R., Valderrama, P., Scao, V., 2016. The eruptive chronology of the Ampato-Sabancaya volcanic complex (Southern Peru). *J. Volcanol. Geotherm. Res.* 323, 110–128.
- Steiger, R.H., Jaeger, E., 1977. Subcommittee on geochronology: Convention on the use of decay constants in geo and cosmochronology. *Earth Plan. Sci. Lett.* 36, 359–362.
- Stern, C.R., 2004. Active Andean volcanism: its geologic and tectonic setting. *Revista Geológica de Chile* 2, 161–206.
- Sun, S., McDonough, W., 1989. Chemical and isotopic systematics of oceanic basalts: Implications for mantle compositions and processes. In: Saunders, A., Norry, M. (Eds.), *Magmatism in Ocean Basins: Geol. Soc. vol. 42. Sp. Publication*, London, pp. 313–345.
- Thouret, J.C., 1999. Volcanic geomorphology, an overview. *Earth Sci. Rev.* 47, 95–131.
- Thouret, J.C., Wörner, G., Singer, B., Legeley-Padovani, A., 2004. “Old” valleys in a “young” mountain range. Published abstract and poster, IA VCEI General Assembly, Pucon Chili 14–19.
- Thouret, J.C., Wörner, G., Gunnell, Y., Singer, B., Zhang, X., Souriot, T., 2007. Geochronologic and stratigraphic constraints on canyon incision and Miocene uplift of the Central Andes in Peru. *Earth Planet. Sci. Lett.* 263, 151–166.
- Wilson, M., 1989. *Igneous Petrogenesis, a Global Tectonic Approach*: Springer. The Netherlands, Dordrecht, p. 457.